NEOPLASIA
www.neoplasia.com

Volume 18 Number 9 September 2016 pp. 567–576 567

Hypoxia-Inducible Factor 2α Mutation-Related Paragangliomas Classify as Discrete Pseudohypoxic Subcluster[1,2]

Stephanie M.J. Fliedner[*,†], Uma Shankavaram[‡], Geena Marzouca[†], Abdel Elkahloun[§], Ivana Jochmanova[†,‖], Roland Daerr[†,¶¶], W. Marston Linehan[¶], Henri Timmers[#], Arthur S. Tischler[**], Konstantinos Papaspyrou[††], Jürgen Brieger[††], Ronald de Krijger[‡‡,§§], Jan Breza[‖‖], Graeme Eisenhofer[¶¶], Zhengping Zhuang[##], Hendrik Lehnert[*] and Karel Pacak[†]

[*]1st Department of Medicine, University Medical Center Schleswig-Holstein, Campus Lübeck, Lübeck, Germany; [†]Section of Medical Neuroendocrinology, *Eunice Kennedy Shriver* National Institute of Child Health and Human Development, National Institutes of Health, Bethesda, MD, USA; [‡]Radiation Oncology Branch, National Cancer Institute, National Institutes of Health, Bethesda, MD, USA; [§]Cancer Genetics Branch, National Human Genome Research Institute, National Institutes of Health, Bethesda, MD, USA; [‖]1st Department of Internal Medicine Medical Faculty of P. J. Šafárik University in Košice, Košice, Slovakia; [¶]Urologic Oncology Branch, Center for Cancer Research, National Cancer Institute, National Institutes of Health, Bethesda, MD, USA; [#]Department of Internal Medicine, Radboud University Medical Centre, Nijmegen, The Netherlands; [**]Tufts Medical Center, Boston, MA, USA; [††]Department of Otorhinolaryngology, Head and Neck Surgery, University Medical Center of the Johannes Gutenberg University Mainz, Mainz, Germany; [‡‡]Department of Pathology, Josephine Nefkens Institute, Erasmus MC-University Medical Center, Rotterdam, The Netherlands; [§§]Department of Pathology, Reinier de Graaf Hospital, Delft, The Netherlands; [‖‖]Department of Urology, Comenius University, Bratislava, Slovak Republic; [¶¶]Institute of Clinical Chemistry & Laboratory Medicine and Department of Medicine III, University Hospital Carl Gustav Carus, Medical Faculty Carl Gustav Carus, Technische Universität Dresden, Dresden, Germany; [##]Surgical Neurology Branch, National Institute of Neurological Disorders and Stroke, National Institutes of Health, Bethesda, MD, USA

Abstract

Recently, activating mutations of the hypoxia-inducible factor 2α gene (*HIF2A*/*EPAS1*) have been recognized to predispose to multiple paragangliomas (PGLs) and duodenal somatostatinomas associated with polycythemia, and ocular abnormalities. Previously, mutations in the *SDHA/B/C/D, SDHAF2, VHL, FH, PHD1*, and *PHD2* genes have been associated with HIF activation and the development of pseudohypoxic (cluster-1) PGLs. These tumors overlap in terms of tumor location, syndromic presentation, and noradrenergic phenotype to a certain extent. However, they also differ especially by clinical outcome and by presence of other tumors or abnormalities. In the present study,

Address all correspondence to: Stephanie Fliedner, Ph.D., Research Lab on Neuroendocrine Oncology, 1st Department of Medicine, University Medical Center Schleswig-Holstein, Campus Lübeck, Ratzeburger Allee 160, 23538 Lübeck, Germany or Karel Pacak, M.D., Ph.D., D.Sc., Section of Medical Neuroendocrinology, *Eunice Kennedy Shriver* National Institute of Child Health and Human Development, National Institutes of Health, 10 Center Dr., Bldg. 10 CRC, Rm. 1E-3140, 20814 Bethesda, MD, USA.
E-mail: stephanie.fliedner@uksh.de

[1] Support: This study was funded by the Eunice Kennedy Shriver National Institute of Child Health and Human Development, National Institutes of Health, Bethesda, MD, USA.
[2] Disclosure statement: The authors have nothing to disclose.
Received 19 April 2016; Revised 22 July 2016; Accepted 25 July 2016

1476-5586
http://dx.doi.org/10.1016/j.neo.2016.07.008

we aimed to establish additional molecular differences between *HIF2A* and non-*HIF2A* pseudohypoxic PGLs. RNA expression patterns of *HIF2A* PGLs ($n = 6$) from 2 patients were compared with normal adrenal medullas ($n = 8$) and other hereditary pseudohypoxic PGLs (*VHL*: $n = 13$, *SDHB*: $n = 15$, and *SDHD*: $n = 14$). Unsupervised hierarchical clustering showed that *HIF2A* PGLs made up a separate cluster from other pseudohypoxic PGLs. Significance analysis of microarray yielded 875 differentially expressed genes between *HIF2A* and other pseudohypoxic PGLs after normalization to adrenal medulla (false discovery rate 0.01). Prediction analysis of microarray allowed correct classification of all *HIF2A* samples based on as little as three genes (*TRHDE, LRRC63, IGSF10*; error rate: 0.02). Genes with the highest expression difference between normal medulla and *HIF2A* PGLs were selected for confirmatory quantitative reverse transcriptase polymerase chain reaction. In conclusion, *HIF2A* PGLs show a characteristic expression signature that separates them from non-*HIF2A* pseudohypoxic PGLs. Unexpectedly, the most significantly differentially expressed genes have not been previously described as HIF target genes.

Neoplasia (2016) 18, 567–576

Introduction

Within the last 5 years, the number of gene mutations associated with paragangliomas (PGLs) and pheochromocytomas (i.e., adrenal PGLs) has more than doubled [1]. Strong genotype-phenotype associations including syndromic presentation; tumor location; malignant potential; and biochemical, metabolomic, and specific imaging phenotypes have been recognized, indicating the need for identification of individualized treatment approaches to hereditary PGLs [2–4].

At the gene expression level, two main groups of PGLs have been identified: those showing increased expression of hypoxia-related genes (pseudohypoxic PGLs, also referred to as cluster-1) and kinase signaling genes (cluster-2) [5–7]. Cluster identity of paragangliomas can be well determined based on metanephrine production because almost exclusively cluster-2 paragangliomas produce metanephrine. Regardless of cluster classification, a current concept suggests that inappropriately elevated HIF signaling may be involved in tumorigenesis of most mutation-derived PGLs [8]. Qin et al. showed that joint HIF-1α and HIF-2α stabilization is predominant in all pseudohypoxic PGLs [9].

A recent addition to the list of gene mutations predisposing to pseudohypoxic PGLs are gain-of-function mutations of hypoxia-inducible factor 2 alpha (*HIF2A* or *EPAS1*) [10]. *HIF2A* PGLs are most often multifocal and recurrent, produce norepinephrine, and occur more frequently in females than males (summarized in [11]). At least half of the afflicted patients reported to date show syndromic presentation including polycythemia from early childhood, PGLs at young age, duodenal somatostatinomas [10,12], and ocular abnormalities [13]. Recently, somatic *HIF2A* mutations have also been detected in central nervous system hemangioblastomas [14] and duodenal gangliocytic PGLs [15], a rare type of tumor composed of neurons, Schwann cells, and enteric-type neuroendocrine cells that differs from true PGLs by expression of keratins, pancreatic polypeptide, and other intestinal regulatory peptides. In the majority of cases, the mutations were found to be somatic and postzygotic; however, rarely, germline mutations as well as germline mosaicism have also been reported [16,17].

PGLs have not been previously associated with a comparable syndromic presentation except for cases of von Hippel–Lindau syndrome, in which almost always adrenal PGLs rarely co-occur with polycythemia and/or somatostatinomas [18,19]. Somatostatinomas have previously been associated with other neuroendocrine syndromes caused by mutations which predispose to cluster-2 PGLs, i.e., multiple endocrine neoplasia 2B (i.e., *RET* mutations) [20] and neurofibromatosis 1 (*NF1* mutations) [21,22]. Nevertheless, in previous studies, the mRNA expression profiles of nine cases of *HIF2A*-mutated PGLs from patients with and without syndromic presentation clustered with other pseudohypoxic PGLs [23–26], whereas, surprisingly, three cases showed more common expression patterns with cluster-2 PGLs [24]. The authors mentioned that several of the reported *HIF2A* tumors were suspected to carry somatic *NF1* mutations; thus, possibly, these three samples were afflicted with both mutations. *HIF2A* expression was increased even in the latter cases compared with cluster-2 PGLs.

Based on distinct clinical presentations of patients with *HIF2A* syndrome from patients with other HIF-stabilizing mutations, differences in the tumor biology and clinical outcome are evident. Despite the fact that stabilization of HIF-1α and/or HIF-2α occurs due to mutations in any cluster-1 tumor susceptibility genes, clinical manifestations and outcomes vastly differ. Particularly for patients with *HIF2A* mutations, who often present early with polycythemia and have a high risk to develop metastatic somatostatinomas and less frequently metastatic PGL and ocular abnormalities, the development of new, targeted approaches to therapy is of the essence. To further elaborate if and how *HIF2A*-related PGLs differ from non-*HIF2A* pseudohypoxic PGLs (e.g., *SDHx* and *VHL*) on the molecular level and to identify potentially druggable targets, we performed a differential gene expression analysis of cluster-1 PGLs.

Results

Identification of a Differentiating Expression Signature in HIF2A PGLs

Principal component analysis showed that *HIF2A* tumor samples have distinct expression characteristics from non-*HIF2A* pseudohypoxic PGLs (Figure 1*A*). In agreement with that, unsupervised hierarchical clustering showed that *HIF2A* PGLs make up a separate subcluster (cluster-1Ab) within the previously described cluster-1A (i.e., a joint cluster of *SDHB* and *SDHD*-abdominal/thoracic [AT] PGLs, which is clearly distinguishable from cluster-1B, containing *VHL* and *SDHD* head and neck PGLs [HNPs] in two distinct subclusters [27]) (Figure 1*B*). Significance analysis of microarray with two-class option at a false discovery rate ≤ 0.01 revealed 875 differentially expressed genes in *HIF2A* PGLs compared with non-*HIF2A* pseudohypoxic PGLs after normalization to normal

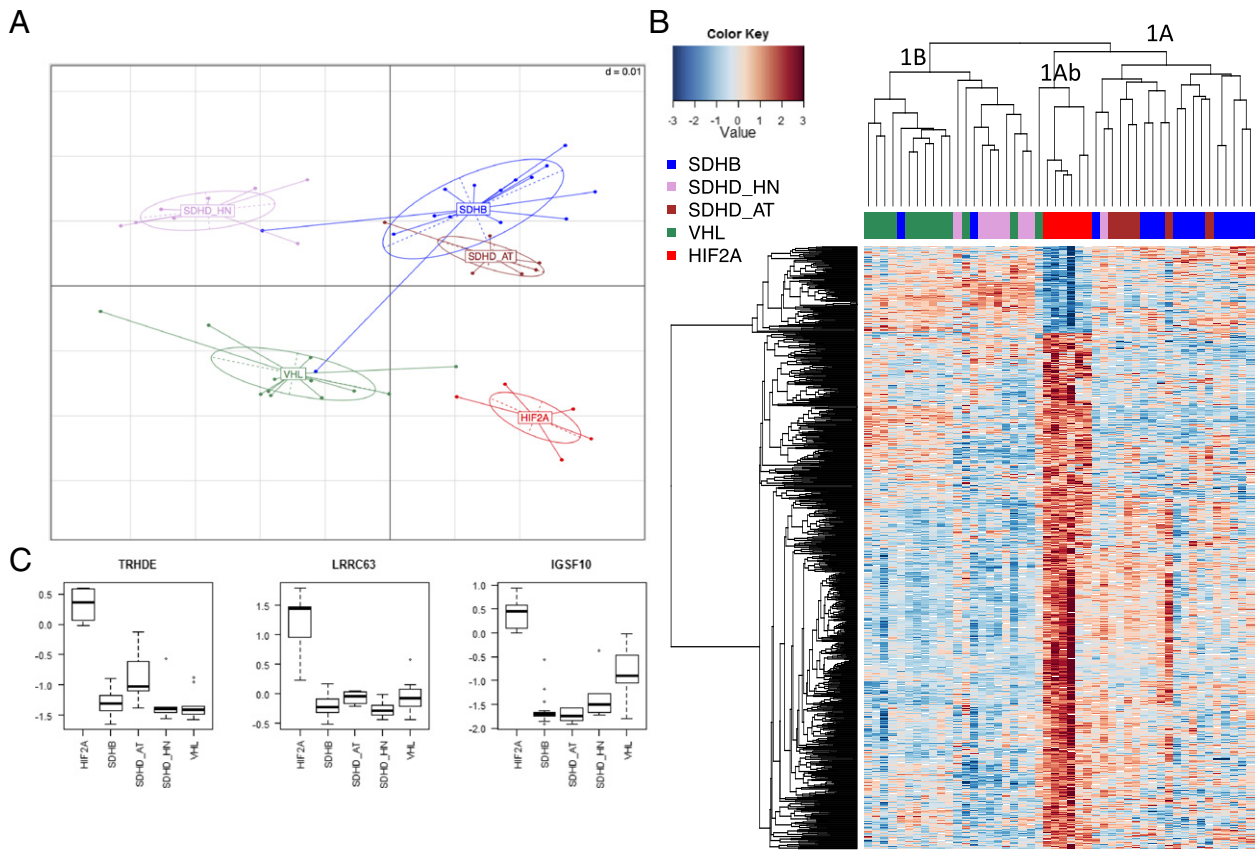

Figure 1. Distinct expression pattern of *HIF2A* PGLs. (A) Principal component analysis showed that *HIF2A* PGLs are clearly distinguishable from other pseudohypoxic PGLs based on their expression pattern. (B) Hierarchical clustering of all pseudohypoxic PGLs based on differentially expressed genes observed by significance analysis of microarray showed separate subclustering of *HIF2A* PGLs in the previously described cluster-1A (a mixed cluster of *SDHB* and *SDHD*-AT PGLs). (C) Top three genes, which allow correct classification of *HIF2A* PGLs with an excellent error rate of merely 2%. The *y*-axis indicates relative gene expression to normal adrenal medulla. Median, first, and third quartiles of relative expression *z*-scores of the gene in question are indicated by midline, bottom, and top of the boxes. Whiskers indicate lowest and highest expression values within 1.5 interquartile ranges of the lower and upper quartile, respectively. Extreme values are depicted as dots and may be considered outliers.

adrenal medulla (Figure 1*B*). Of these 875 genes, 96 were 1.5-fold more highly expressed in *HIF2A* than non-*HIF2A* pseudohypoxic PGLs, whereas 27 were 1.5-fold more highly expressed in the latter (Table S1).

Prediction analysis of microarray at a threshold of 2.3 allowed correct classification of all *HIF2A* samples based on 354 genes with only one misclassification of an *SDHD* adrenal PGL (D31.1) with an error rate of 0.02 (Table 1). Correct classification among cluster-1 PGLs with this low error rate was even achieved based on the expression of just three genes: *TRHDE, LRRC63*, and *IGSF10* (Figure 1*C*).

HIF-α Target Gene Signature

Comparison of previously reported HIF-1α and HIF-2α target gene lists with the 875 genes, which were identified to be differentially expressed between *HIF2A* and other pseudohypoxic PGLs by significance analysis of microarray, led to few or no matches (0%-8.3%; 0/72 [28], 20/443 [29], 2/24 [30], 7/117 [31–33], 21/500 [34]). There was no preference for either HIF-1α or HIF-2α target genes. When a fold change (FC) threshold equal or greater than 1.5 or equal or less than −1.5 was chosen, only two reported HIF-1α target genes (*MIF*: FC = 1.6, *FLT1*: FC = −1.7), two HIF-1α and HIF-2α target genes (*KRT19*: FC = 1.8, *PDK1*: FC = −1.56), and one HIF-2α target gene remained (*PRKCA*: FC = −1.59). Surprisingly, the expression of the HIF-2α target gene *PRKCA* was significantly decreased in *HIF2A* PGLs compared with all other groups.

Moreover, *MIF* and *FLT1* expression changes were in opposing directions, with *MIF* being more highly expressed in *HIF2A* than all other groups except for SDHD-AT and *FLT1* being expressed at similar levels in *HIF2A* and normal medulla while being elevated in all other groups (Figure 2*A*). Similarly, *KRT19* and *PDK1* were changed in opposing directions. *KRT19* was downregulated in all pseudohypoxic PGLs compared with normal medulla and *HIF2A* samples, whereas PDK1 was downregulated in *HIF2A* compared with normal medulla, *SDHB* and *VHL* PGLs.

Overall, these findings may indicate that the hypoxic expression signatures of *HIF2A* and other pseudohypoxic PGLs are mainly in

Table 1. Confusion matrix for classification of HIF-2α samples

	HIF2A	Other Pseudohypoxic	Error Rate
HIF2A	6	0	0.00
Other pseudohypoxic	1	41	0.02
	Overall error rate=		0.02

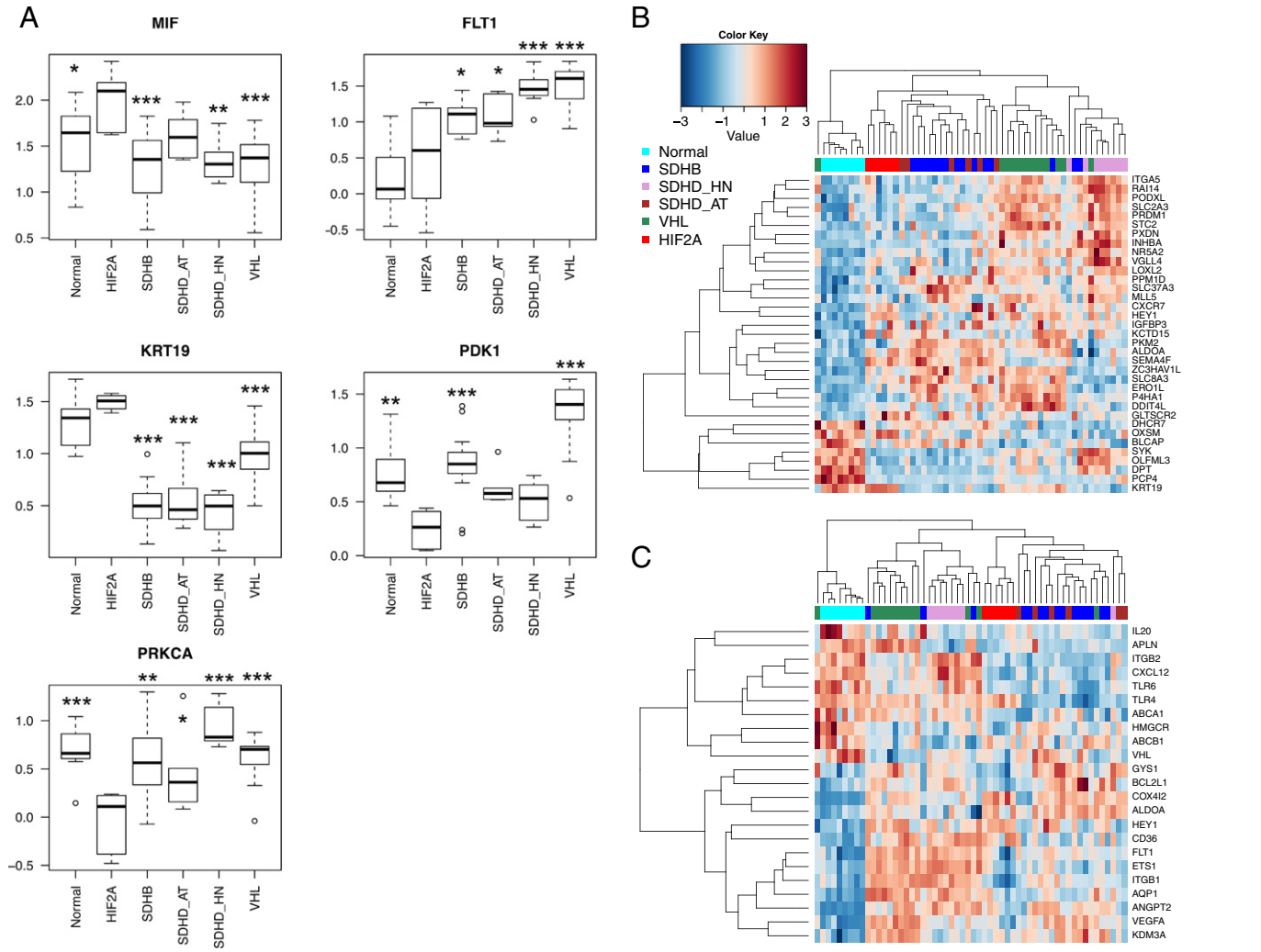

Figure 2. HIF target gene expression in pseudohypoxic PGLs. (A) Five HIF target genes, which were identified to be differentially expressed between *HIF2A* and other pseudohypoxic PGLs. The *y*-axis indicates normalized gene expression level. Median, first, and third quartiles of normalized expression *z*-scores of the gene in question are indicated by midline, bottom, and top of the boxes. Whiskers indicate lowest and highest expression values within 1.5 interquartile ranges of the lower and upper quartile, respectively. Extreme values are depicted as dots and may be considered outliers. Overall ANOVA was performed. Asterisks indicate significantly different expression from *HIF2A* as determined by *post hoc* analysis using Dunnett's test (***$P \leq .001$, **$P \leq .01$, *$P \leq .05$). (B and C) Upon restriction of the 1721 differentially expressed genes between normal medulla and pseudohypoxic PGLs to those that have been previously reported as HIF target genes, separate clustering of *HIF2A* PGLs was maintained, indicating differences in HIF target gene activation between the *HIF2A* PGLs and other pseudohypoxic PGLs. HIF target genes presented in B are from the transcription factor encyclopedia, and those shown in C are from [29].

agreement as previously suggested and that general upregulation of HIF signaling is a common denominator [5,7,35].

To evaluate the overlap in expression between *HIF2A* and non-*HIF2A* pseudohypoxic PGLs, we compared the expression patterns of all pseudohypoxic PGLs combined (including *HIF2A* PGLs) with normal adrenal medulla. Significance analysis of microarray revealed 1721 differentially expressed genes at a *q*-value of 1%. Ingenuity Pathway Analysis (IPA) of the differentially expressed genes between all pseudohypoxic PGLs and normal medulla with an FC greater than 1.5 predicted transcription factor activation, among others, for HIF-1α, HIF-2α, and *ARNT2*, an HIFβ subunit (activation *z*-scores: 2.409, 2.379, and 2.236 and overlap factors: $1.63*10^{-5}$, $1.37*10^{-5}$, and $2.236*10^{-3}$, respectively). Genes and changes in expression which led to the prediction of activation are shown in Table S3. These data suggest that a common activation of both HIF-1α and HIF-2α is likely to be present in all pseudohypoxic PGLs.

Matching the significance analysis of microarray list of differentially expressed genes between normal medulla and all pseudohypoxic PGLs revealed more matches to reported and predicted HIF target gene lists (7.9%-20.1%; 9/72 [28], 35/443 [29], 5/24 [30], 14/117 [31–33], 50/500 [34]). Interestingly, despite similar expression changes in these HIF targets among all pseudohypoxic PGLs compared with normal medulla, hierarchical clustering of all groups with either of those HIF target gene lists led to separate clustering of *HIF2A* PGLs from non-*HIF2A* PGLs in a similar manner as when using all 875 genes (Figure 2, *B* and *C*), indicating that *HIF2A* PGLs are more similar to each other than non-*HIF2A* PGLs overall but also with respect to HIF target genes. Thus, although all pseudohypoxic PGLs show some agreement in their HIF signature, even when

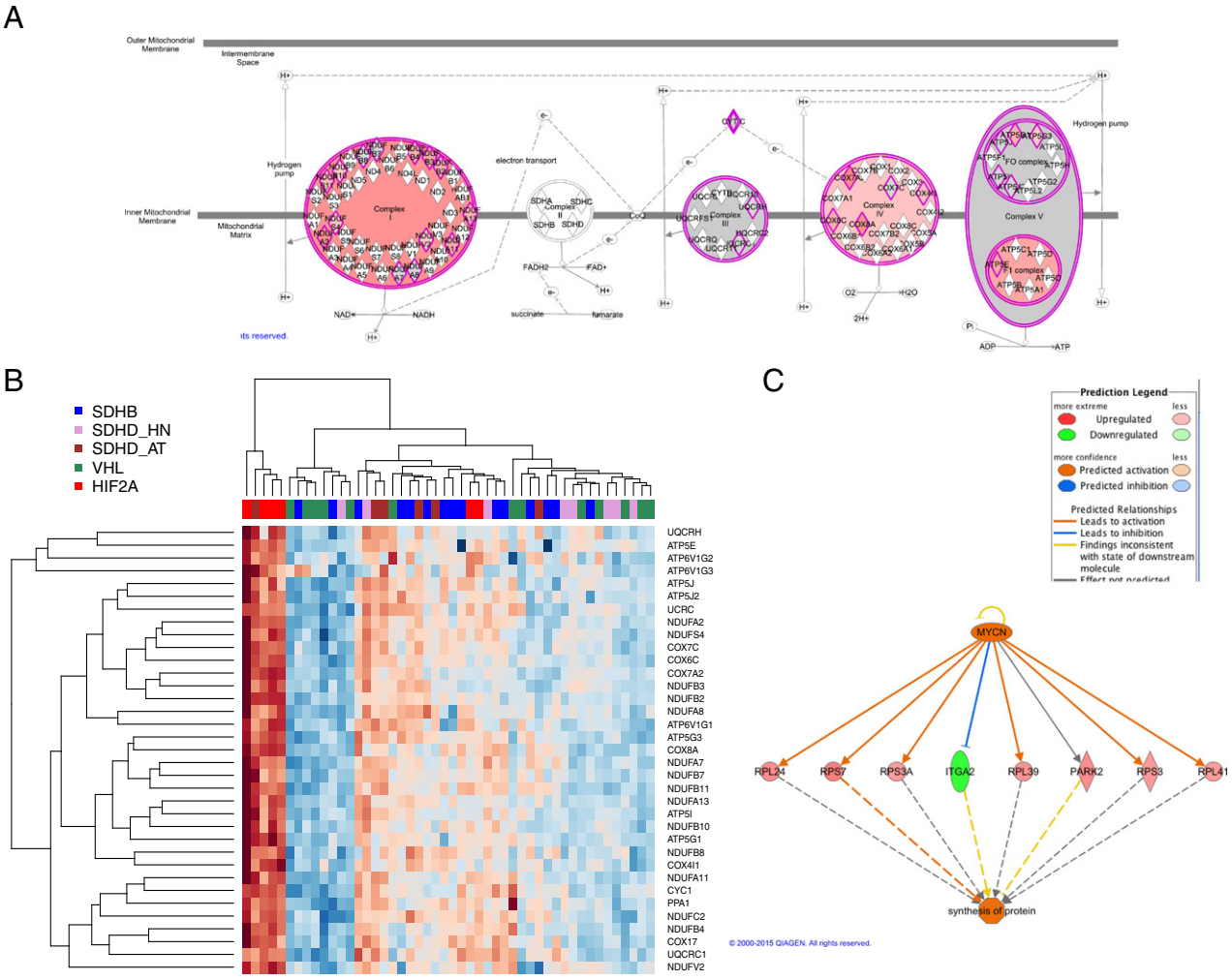

Figure 3. Indication of activated pathways in *HIF2A* PGLs. (A) IPA revealed increased expression of a vast number of genes essential in oxidative phosphorylation in *HIF2A* PGLs (red indicates upregulation in *HIF2A* PGLs compared with pseudohypoxic PGLs). (B) Heatmap depicting upregulation of oxidative phosphorylation genes in *HIF2A* PGLs after comparison of differentially expressed genes in *HIF2A* compared with other pseudohypoxic PGLs with the oxydative phosphorylation genes listed in the Kyoto Encyclopedia of Genes and Genomes (red indicates upregulation). (C) Upregulation of several genes for ribosomal proteins led to prediction of increased protein synthesis and *MYCN* activation in HIF2A PGLs by IPA.

limited to those genes, separation of *HIF2A* PGLs remains possible. This indicates characteristically different nuances of HIF target gene activation in *HIF2A* PGLs.

To focus on unique features of *HIF2A* PGLs on the pathway level, core analysis was performed using IPA. Oxidative phosphorylation was reported as top canonical pathway, with 27 of 93 related genes being more highly expressed in the *HIF2A* group than the group of non-*HIF2A* pseudohypoxic PGLs (Figure 3*A*). This was confirmed by matching the significance analysis of microarray list to the genes listed for oxidative phosphorylation in the Kyoto Encyclopedia of Genes. Upregulation was evident for 35 of 128 listed genes (Figure 3*B*). However, as is visible in Figure 3*B*, very strong upregulation of oxydative phosphorylation genes was predominant in only four of six *HIF2A* samples, which skewed the group median *z*-score. These four samples were all from patient H48. The two other *HIF2A* samples from patient H49 subclustered with five *SDHB* PGLs. Because oxidative phosphorylation was still the top-rated pathway based on group medians of relative expression and we previously showed that *SDHB* and *SDHD*-AT PGLs have stronger expression of oxidative phosphorylation genes than *VHL* and *SDHD*- HNP, we still consider this finding interesting because it reflects that *HIF2A* PGLs may depend less on glycolytic energy metabolism. Another pathway reported to be highly activated was EIF2 signaling, with 32 genes from the pathway being upregulated, including 30 ribosomal proteins. In agreement with that, EIF4E was predicted to be activated based on upregulation of nine genes (Table S3, activation *z*-score = 2.530, overlap *P* value = .046). Furthermore, translation, expression, and synthesis of proteins were suggested to be elevated in *HIF2A* PGLs based on IPA downstream analysis. Interestingly, *MYCN* was predicted to be activated (activation *z*-score = 3.599, overlap *P* value = $1.54*10^{-5}$), which may explain elevated expression of several genes involved in protein synthesis (Figure 3*C*).

Unique Features of HIF2A PGLs

To further specify the characteristic expression signature of *HIF2A* PGLs, we chose a two-step approach using significance analysis of microarray, first identifying the differentially expressed genes between

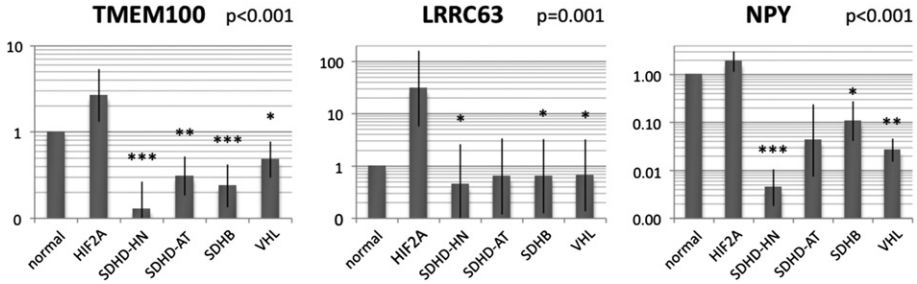

Figure 4. Relative mRNA expression of genes of interest in *HIF2A* compared with other pseudohypoxic PGLs as assessed by validatory qRT-PCR. Expression of the candidate markers for *HIF2A* PGLs, *TMEM100, NPY*, and *LRRC63*, was assessed relative to *RPLP0* in a vastly separate sample set than the one assessed for the microarray. Bars indicate group means ± SEM. Overall ANOVA was performed. Asterisks indicate significantly different expression from HIF2A as determined by *post hoc* analysis using Dunnett's test (***$P \leq .001$, **$P \leq .01$, *$P \leq .05$).

normal adrenal medulla and *HIF2A* PGLs (1240 genes, *q*-value 1%) and then matching it to a list of genes differentially expressed between non-*HIF2A* and *HIF2A* PGLs (254 genes, *q*-value 1%). A heatmap of this characteristic *HIF2A*-PGL expression signature relative to other pseudohypoxic PGLs is given in Figure S2 and the genes are listed in Table S3.

Genes of Interest

Ten genes of interest were chosen for further exploration by rating the 875 genes we found to be differentially expressed between *HIF2A* and other pseudohypoxic PGLs based on the magnitude of difference in expression between normal adrenal medulla and *HIF2A* PGLs and a false discovery rate below 0.01 in significance analysis of microarray. Quantitative reverse transcriptase polymerase chain reaction (qRT-PCR) for a largely separate set of PGL samples was performed for 9 of the 10 genes of interest and essentially confirmed the microarray data for 6 genes ($P \leq .001$: *TMEM100, NPY*, and *LRRC63; *$P \leq .05$: *PTN, GNG11, IL20RA*). The three genes most likely to qualify to distinguish *HIF2A* PGLs from other pseudohypoxic PGLs were thus *TMEM100, NPY*, and *LRRC63* (Figure 4), and they potentially play distinguishing roles in *HIF2A* PGL tumor biology.

Previously, pseudohypoxic PGLs have been reported to be highly vascular and exhibit increased VEGF signaling [36]. Toledo et al. reported similar expression of *VEGFA* in two cases of *HIF2A* PGLs and cluster-1 PGLs, which was significantly higher than in cluster-2 PGLs [26]. Within our cohort, VEGFA expression was increased compared with normal medulla in all pseudohypoxic PGL groups but to a lesser extent in HIF2A than the other groups. Expression of the VEGF receptors, *NRP1* (*VEGF165R*), *KDR* (*VEGFR-2*), and *FLT1* (*VEGFR-1*), was at similarly low or lower levels in *HIF2A* PGLs compared with normal medulla. Gene expression was significantly elevated in *SDHD*-HN and *VHL* PGLs (KDR); *SDHB, VHL*, and *SDHD*-HN PGLs (NRP1); or *SDHB, SDHD*-AT, *SDHD*-HN, and *VHL* PGLs (*FLT1*) compared with *HIF2A* samples (Figure S1).

Discussion

Our gene expression data based on 48 pseudohypoxic PGLs and 8 normal adrenal medullas indicate that *HIF2A* PGLs show expression features that on the one hand unite and on the other hand clearly distinguish them from non-*HIF2A* pseudohypoxic PGLs.

In support of significant differences in gene expression profiles of *HIF2A* and non-*HIF2A* pseudohypoxic PGLs, correct classification of *HIF2A* PGLs was excellent.

Characteristic expression of *TRHDE, LRRC63*, and *IGSF10* was sufficient to correctly classify all *HIF2A* PGL samples. In our cohort, *LRRC63* was more highly expressed in *HIF2A* PGL samples than all other tissues, including normal medulla. Thus, *LRRC63* may play an essential role in *HIF2A* PGL development. Currently, the function of *LRRC63* is unknown.

Our data further show decreased expression of *IGSF10* and *TRHDE* in all non-*HIF2A* pseudohypoxic tumors relative to normal medulla and *HIF2A* PGLs. Interestingly, *TRHDE* has been shown to be hypermethylated in oral squamous cell cancers and dysplastic tissue compared with adjacent normal tissue [37], which generally leads to decreased transcription. In addition, *IGSF10* has been described to be downregulated in radiation-induced rat osteosarcomas relative to normal osteoblasts [38]. Thus, decreased *TRHDE* and *IGSF10* expression, possibly caused by hypermethylation, may contribute to tumorigenesis in non-*HIF2A* pseudohypoxic PGLs.

Nevertheless, *HIF2A*-initiated transcription does not seem to play a major role in the observed differential expression patterns. Our data showed minimal overlap of differentially expressed genes between *HIF2A* and non-*HIF2A* pseudohypoxic PGLs with previously published HIF target gene lists. Comparison of the combined expression patterns of all pseudohypoxic PGLs (including *HIF2A*) relative to normal adrenal medulla indicated differential expression of almost always twice as many HIF target genes upon comparison with published and predicted HIF target gene lists [28–34]. This confirms previous reports suggesting a common HIF pathway-related expression signature for all pseudohypoxic PGLs [5,7,35].

Selected *HIF2A* target genes, however, did show differences in expression level between the analyzed pseudohypoxic PGLs, indicating that slight differences in HIF target gene expression exist and may contribute to the variation in manifestation between the analyzed tumor groups. The *HIF1A* and *HIF2A* target gene *KRT19* is a key player in epithelial to mesenchymal transition and has been reported to be expressed in neuroendocrine tumors [39]. In addition, it is used as a marker to detect circulating breast cancer cells and correlates with highly proliferating tumors and the risk for metastases [40]. On the contrary, epigenetic downregulation of KRT19 in SDHB-PGLs has been shown [41,42], and its downregulation

contributed to increased cell motility and invasiveness. In our cohort, *HIF2A* PGLs showed similar *KRT19* expression compared with normal medulla and decreased expression in the other pseudohypoxic PGLs. In agreement with that, Toledo et al. showed increased mRNA expression of *KRT19* in a *HIF2A* PGL compared with cluster-1 and cluster-2 PGLs [26]. *KRT19* mRNA expression at similar level as seen in the normal medulla may reflect reduced aggressiveness with slower tumor progression observed in our *HIF2A* patient cohort compared with, e.g., SDHB patients.

Exploration of concerted changes in gene expression in *HIF2A*-related PGLs revealed oxidative phosphorylation and protein translation/synthesis to be upregulated compared with non-*HIF2A* pseudohypoxic PGLs. We previously showed increased expression of several oxidative phosphorylation genes, but in a less concerted manner, in *SDHB* and *SDHD*-AT PGLs compared with *VHL* and *SDHD*-HN PGLs [27,43]. *HIF2A* PGLs from patient H48 showed even higher levels of oxidative phosphorylation gene expression, whereas those of H49 fell into a subcluster shared with five *SDHB* PGLs, which we previously showed to have a tendency for higher expression of oxidative phosphorylation genes, and surprisingly one *SDHD*-HN PGL. Thus, expression of oxydative phosphorylation genes may be very strong in certain *HIF2A* PGLs while being comparable to other pseudohypoxic PGLs in others.

Dysfunction of VHL has been reported to cause decreased oxidative phosphorylation complex subunit expression [44] by way of HIF signaling and reactive oxygen species generation [45]. Dysfunction of the SDH complex has been previously associated with reactive oxygen species generation [46–48] and may thus share a similar mechanism of oxidative phosphorylation gene downregulation for certain mutations. Hervouet et al. [44] used cells which do not express HIF-1α and showed that presence of HIF-2α is essential in downregulation of oxidative phosphorylation genes. In contrast, using the same cell model, Biswas et al. showed that HIF-1α overexpression (with a background of endogeneous HIF-2α) led to a decreased level of mitochondrial activity, whereas HIF-2α overexpression (in absence of HIF-1α) induced mitochondrial activity [49]. In agreement with that, Chiavarina et al. showed that HIF-2α activity increased oxidative phosphorylation gene expression, whereas it was decreased by HIF-1α activity [50]. In *HIF2A* PGLs, activation of HIF-1α is absent or minimal [12,51], and thus, a similar picture as seen in the model systems of Biswas and Chiacarina may be present in those tumors, whereas in the other pseudohypoxic tumors, likely a simultaneous activation of HIF-2α and HIF-1α is present [9].

Determination of oxidative phosphorylation function in *HIF2A* compared with non-*HIF2A* PGLs or in appropriate PGL cell models is needed to confirm differential regulation of oxidative phosphorylation by HIF-1α and HIF-2α stabilization. Increased expression of oxidative phosphorylation genes in some *HIF2A* PGLs may indicate that these tumors are not as dependent on the Warburg effect as other pseudohypoxic PGLs. In agreement with that, our own unpublished observations indicate that imaging of elevated glucose turnover via 18-fluoro-deoxyglucose is much less specific for *HIF2A* PGLs than for other pseudohypoxic PGLs, especially those with *SDHB* mutations.

Protein translation has previously been reported to be inhibited by hypoxia [52], abnormal pVHL [53], and PHD2 [54]. Thus, decreased protein translation in pseudohypoxic PGLs with PHD2 or VHL dysfunction as well as inhibited PHDs due to *SDHx* mutations would be expected. Our results show higher expression of 43 ribosomal proteins in *HIF2A* PGLs compared with the other pseudohypoxic PGLs, indicating that, as discussed above, exclusive HIF-2α stabilization may have effects that differ from general hypoxia or stabilization of all HIF-α subunits.

We identified potential *HIF2A* PGL markers with distinct expression in *HIF2A* PGLs compared with the other pseudohypoxic PGLs. Of those, *TMEM100, LRRC63*, and *NPY* best qualified as characteristically expressed in *HIF2A* PGLs. TMEM100 is essential for epithelial to mesenchymal transition [55], which is required for maturation and migration of neural crest precursors. In hepatocellular carcinomas, a tumor suppressor role of TMEM100 by inhibition of proliferation and metastatic spread has been described [56]. In agreement, lack of TMEM100 induces *VEGFA* expression in myocardial cells [55]. In the *HIF2A* PGLs, we noticed higher *TMEM100* levels and lower *VEGFA* expression compared with other pseudohypoxic PGLs, in which the opposite pattern was observed. Moreover, the VEGF receptors *NRP1, KDR*, and *FLT1* were expressed at lower levels in adrenal medulla and *HIF2A* PGLs compared with most non-*HIF2A* PGLs. Thus, *HIF2A* PGLs may be less susceptible to antiangiogenic treatment than other pseudohypoxic PGLs.

NPY has been previously shown to be more highly expressed in adrenergic than noradrenergic or *RET*- than *VHL*-mutated pheochromocytomas [57]. Here we observed *NPY* expression that was increased in *HIF2A* PGLs compared with all other pseudohypoxic PGLs. Toledo et al. showed decreased expression of *NPY* in an *HIF2A* PGL compared with *NF1* and possibly *VHL* PGLs, whereas expression level appears similarly low in *SDHB* as in the *HIF2A* sample [26].

In conclusion, *HIF2A* PGLs share certain features of pseudohypoxic PGLs; however, they are also truly distinct. This may be related to a somewhat different activation pattern of HIF target genes, oxidative phosphorylation genes, as well as angiogenesis-related genes. In addition to the indication that *HIF2A* PGLs are less vascular and less affected by oxidative phosphorylation dysfunction than other pseudohypoxic PGLs, they also show elevated expression of NPY, protein transcription, and MYCN activation genes, as has been shown for cluster-2 PGLs. Thus, unique or even cluster-2–like expression aspects of *HIF2A* PGLs will have to be factored in when developing new treatment strategies for *HIF2A* PGLs.

Material and Methods

All tumor and normal tissue samples were collected and processed with informed patient consent as previously reported [27]. Normal adrenal medulla was microdissected from cortex under microscopic guidance as previously described [58]. In addition to the previously reported samples, material of six *HIF2A* tumors from two different female patients (H48 and H49) were used. Patient H48 underwent surgery at the age of 29 and had 4 paragangliomas and 2 somatostatinomas removed. The patient later developed asynchronous bilateral pheochromocytomas and additional paragangliomas as well as somatostatinomas with corresponding metastases. Patient H49 had a pheochromocytoma and a paraganglioma removed at the age of 18. Within the same year, somatostatinomas of the pancreas and duodenum were resected. Patient information is given in Table 2.

Table 2. Tissue sample information

	Mutation	Sex	Age at Surgery	Tissue Type	Status
N01	dna	m	61	normal	dna
N02	dna	nk	nk	normal	dna
N03	dna	f	53	normal	dna
N04–1	dna	f	72	normal	dna
N0–2	dna	f	72	normal	dna
N05	dna	m	65	normal	dna
N06	dna	m	56	normal	dna
N07	dna	m	62	normal	dna
B08	SDHB	f	30	PHEO	Pr-NM
B10	SDHB	m	24	PGL	Pr-M
B12	SDHB	f	9	PGL	Mlt-NM
B14	SDHB	m	27	PGL	Met
B15	SDHB	m	38	PGL	Pr-M
B16	SDHB	f	47	PGL	Mlt-NM
B17–1	SDHB	f	36	PGL	Met
B17–2	SDHB	f	36	PGL	Met
B18	SDHB	m	52	PGL	Met
B19	SDHB	m	12	PGL	Pr-NM
B20	SDHB	m	31	PGL	Pr-NM
B21	SDHB	m	55	PGL	Mlt-NM
B22	SDHB	m	35	PGL	Mlt-NM
B23	SDHB	f	35	PGL	Met
B24	SDHB	m	17	PHEO	Mlt-NM
D25	SDHD	m	24	HNP	Pr-NM
D26	SDHD	f	34	HNP	Bi-M
D27	SDHD	f	49	HNP	Pr-NM
D28	SDHD	f	61	HNP	Pr-NM
D29	SDHD	m	16	PHEO	Pr-NM
D30	SDHD	f	31	PHEO	Pr-NM
D31–1	SDHD	f	27	PHEO	Mlt-NM
D31–2	SDHD	f	27	HNP	Mlt-NM
D31–3	SDHD	f	27	HNP	Mlt-NM
D32	SDHD	m	48	HNP	Bi-NM
D33	SDHD	m	61	PHEO	Pr-NM
D44	SDHD	f	29	HNP	Mlt-NM
D35–1	SDHD	m	32	PHEO	Mlt-NM
D35–2	SDHD	m	33	PGL	Mlt-NM
V36	VHL	f	25	PHEO	Bi-NM
V37–1	VHL	m	23	PHEO	Bi/Mlt-NM
V37–2	VHL	m	23	PHEO	Bi/Mlt-NM
V38	VHL	M	16	PHEO	Bi/Rec-NM
V39	VHL	m	29	PHEO	Pr-NM
V40	VHL	m	13	PHEO	Bi-NM
V41	VHL	f	43	PHEO	Pr-NM
V42	VHL	m	29	PHEO	Bi/Mlt-NM
V43	VHL	f	43	PHEO	Bi-NM
V44	VHL	m	39	PHEO	Pr-NM
V45	VHL	m	31	PHEO	Bi-NM
V46	VHL	m	33	PHEO	Bi/Mlt/Rec-NM
V47	VHL	m	19	PHEO	Bi/Mlt-NM
H48–1	HIF2A	f	29	PGL	Mlt-NM
H48–4	HIF2A	f	29	PGL	Mlt-NM
H48–5	HIF2A	f	29	PGL	Mlt-NM
H48–6	HIF2A	f	29	PGL	Mlt-NM
H49–1	HIF2A	f	18	PHEO	Mlt-NM
H49–2	HIF2A	f	18	PGL	Mlt-NM

Abbreviations: *dna*, does not apply; *f*, female; *m*, male; *nk*, not known; *PGL*, paraganglioma; *PHEO*, pheochromocytoma (i.e. adrenal PGL); *HNP*, head and neck paraganglioma; *pr*, solitary PHEO/PGL; *mlt*, multiple PGLs; *bi*, bilateral PHEO; *m*, metastatic disease; *met*, metastases; *nm*, nonmetastatic disease.

GeneChip Human Gene 1.0 ST Array (Affymetrix)

"Core" probe sets were used to perform "gene-level" probe set summarization, background subtraction, and quantile normalization using the RMA option in Expression Console 1.0 (Affymetrix). Data analysis was performed using R packages from the Bioconductor project (http://www.bioconductor.org), as previously described [27].

Differential expression analysis was done by significance analysis of microarray. Class prediction analysis using prediction analysis for microarray was done to predict the genotypes.

IPA

Data were analyzed through the use of QIAGEN's IPA (QIAGEN Redwood City, www.qiagen.com/ingenuity).

qRT-PCR for Genes of Interest

qRT-PCR was performed for nine genes of interest using Taqman primer/probes (Life Technologies, Table S1) on a widely independent sample set of *HIF2A* (n = 6), *SDHB* (n = 9), *SDHD* (n = 12), *VHL* (n = 10), and normal adrenal medulla (n = 5). Patient information is given in Table S2.

Acknowledgements

We would like to thank Dr. Dimitrios Koutsimpelas for his help with retrieving patient information.

Appendix A. Supplementary data

Supplementary data to this article can be found online at http://dx.doi.org/10.1016/j.neo.2016.07.008.

References

[1] Jochmanova I, Zhuang Z, and Pacak K (2015). Pheochromocytoma: gasping for air. *Horm Cancer* **6**, 191–205.

[2] Rao JU, Engelke UF, Sweep FC, Pacak K, Kusters B, Goudswaard AG, Hermus AR, Mensenkamp AR, Eisenhofer G, and Qin N, et al (2015). Genotype-specific differences in the tumor metabolite profile of pheochromocytoma and paraganglioma using untargeted and targeted metabolomics. *J Clin Endocrinol Metab* **100**, E214-222.

[3] Richter S, Peitzsch M, Rapizzi E, Lenders JW, Qin N, de Cubas AA, Schiavi F, Rao JU, Beuschlein F, and Quinkler M, et al (2014). Krebs cycle metabolite profiling for identification and stratification of pheochromocytomas/paragangliomas due to succinate dehydrogenase deficiency. *J Clin Endocrinol Metab* **99**, 3903–3911.

[4] Eisenhofer G, Lenders JW, Timmers H, Mannelli M, Grebe SK, Hofbauer LC, Bornstein SR, Tiebel O, Adams K, and Bratslavsky G, et al (2011). Measurements of plasma methoxytyramine, normetanephrine, and metanephrine as discriminators of different hereditary forms of pheochromocytoma. *Clin Chem* **57**, 411–420.

[5] Eisenhofer G, Huynh TT, Pacak K, Brouwers FM, Walther MM, Linehan WM, Munson PJ, Mannelli M, Goldstein DS, and Elkahloun AG (2004). Distinct gene expression profiles in norepinephrine- and epinephrine-producing hereditary and sporadic pheochromocytomas: activation of hypoxia-driven angiogenic pathways in von Hippel–Lindau syndrome. *Endocr Relat Cancer* **11**, 897–911.

[6] Dahia PL, Ross KN, Wright ME, Hayashida CY, Santagata S, Barontini M, Kung AL, Sanso G, Powers JF, and Tischler AS, et al (2005). A HIF1alpha regulatory loop links hypoxia and mitochondrial signals in pheochromocytomas. *PLoS Genet* **1**, 72–80.

[7] Favier J, Briere JJ, Burnichon N, Riviere J, Vescovo L, Benit P, Giscos-Douriez I, De Reynies A, Bertherat J, and Badoual C, et al (2009). The Warburg effect is genetically determined in inherited pheochromocytomas. *PLoS One* **4**, e7094.

[8] Jochmanova I, Yang C, Zhuang Z, and Pacak K (2013). Hypoxia-inducible factor signaling in pheochromocytoma: turning the rudder in the right direction. *J Natl Cancer Inst* **105**, 1270–1283.

[9] Qin N, de Cubas AA, Garcia-Martin R, Richter S, Peitzsch M, Menschikowski M, Lenders JW, Timmers HJ, Mannelli M, and Opocher G, et al (2014). Opposing effects of HIF1alpha and HIF2alpha on chromaffin cell phenotypic features and tumor cell proliferation: Insights from MYC-associated factor X. *Int J Cancer* **135**, 2054–2064.

[10] Zhuang Z, Yang C, Lorenzo F, Merino M, Fojo T, Kebebew E, Popovic V, Stratakis CA, Prchal JT, and Pacak K (2012). Somatic HIF2A gain-of-function mutations in paraganglioma with polycythemia. *N Engl J Med* **367**, 922–930.

[11] Jochmanova I, Zelinka T, Widimsky Jr J, and Pacak K (2014). HIF signaling pathway in pheochromocytoma and other neuroendocrine tumors. *Physiol Res* **63**(Suppl 2), S251–S262.

[12] Pacak K, Jochmanova I, Prodanov T, Yang C, Merino MJ, Fojo T, Prchal JT, Tischler AS, Lechan RM, and Zhuang Z (2013). New syndrome of paraganglioma and somatostatinoma associated with polycythemia. *J Clin Oncol* **31**, 1690–1698.

[13] Pacak K, Chew EY, Pappo AS, Yang C, Lorenzo FR, Wilson MW, Aronow MB, Young JA, Popovic V, and Zhuang Z (2014). Ocular manifestations of hypoxia-inducible factor-2alpha paraganglioma-somatostatinoma-polycythemia syndrome. *Ophthalmology* **121**, 2291–2293.

[14] Taieb D, Barlier A, Yang C, Pertuit M, Tchoghandjian A, Rochette C, Zattara-Canoni H, Figarella-Branger D, Zhuang Z, and Pacak K, et al (2016). Somatic gain-of-function HIF2A mutations in sporadic central nervous system hemangioblastomas. *J Neurooncol* **126**, 473–481.

[15] Zhuang Z, Yang C, Ryska A, Ji Y, Hou Y, Graybill SD, Bullova P, Lubensky IA, Kloppel G, and Pacak K (2016). HIF2A gain-of-function mutations detected in duodenal gangliocytic paraganglioma. *Endocr Relat Cancer* **23**, L13–16.

[16] Lorenzo FR, Yang C, Ng Tang Fui M, Vankayalapati H, Zhuang Z, Huynh T, Grossmann M, Pacak K, and Prchal JT (2013). A novel EPAS1/HIF2A germline mutation in a congenital polycythemia with paraganglioma. *J Mol Med* **91**, 507–512.

[17] Buffet A, Smati S, Mansuy L, Menara M, Lebras M, Heymann MF, Simian C, Favier J, Murat A, and Cariou B, et al (2014). Mosaicism in HIF2A-related polycythemia-paraganglioma syndrome. *J Clin Endocrinol Metab* **99**, E369-373.

[18] Karasawa Y, Sakaguchi M, Minami S, Kitano K, Kawa S, Aoki Y, Itoh N, Sakurai A, Miyazaki M, and Watanabe T, et al (2001). Duodenal somatostatinoma and erythrocytosis in a patient with von Hippel–Lindau disease type 2 A. *Intern Med* **40**, 38–43.

[19] Capodimonti S, Teofili L, Martini M, Cenci T, Iachininoto MG, Nuzzolo ER, Bianchi M, Murdolo M, Leone G, and Larocca LM (2012). Von hippel–lindau disease and erythrocytosis. *J Clin Oncol* **30**, e137–e139.

[20] Moline J and Eng C (2011). Multiple endocrine neoplasia type 2: an overview. *Genet Med* **13**, 755–764.

[21] Garbrecht N, Anlauf M, Schmitt A, Henopp T, Sipos B, Raffel A, Eisenberger CF, Knoefel WT, Pavel M, and Fottner C, et al (2008). Somatostatin-producing neuroendocrine tumors of the duodenum and pancreas: incidence, types, biological behavior, association with inherited syndromes, and functional activity. *Endocr Relat Cancer* **15**, 229–241.

[22] Relles D, Baek J, Witkiewicz A, and Yeo CJ (2010). Periampullary and duodenal neoplasms in neurofibromatosis type 1: two cases and an updated 20-year review of the literature yielding 76 cases. *J Gastrointest Surg* **14**, 1052–1061.

[23] Welander J, Andreasson A, Brauckhoff M, Backdahl M, Larsson C, Gimm O, and Soderkvist P (2014). Frequent EPAS1/HIF2alpha exons 9 and 12 mutations in non-familial pheochromocytoma. *Endocr Relat Cancer* **21**, 495–504.

[24] Comino-Mendez I, de Cubas AA, Bernal C, Alvarez-Escola C, Sanchez-Malo C, Ramirez-Tortosa CL, Pedrinaci S, Rapizzi E, Ercolino T, and Bernini G, et al (2013). Tumoral EPAS1 (HIF2A) mutations explain sporadic pheochromocytoma and paraganglioma in the absence of erythrocytosis. *Hum Mol Genet* **22**, 2169–2176.

[25] Favier J, Buffet A, and Gimenez-Roqueplo AP (2012). HIF2A mutations in paraganglioma with polycythemia. *N Engl J Med* **367**, 2161 [author reply 2161-2162].

[26] Toledo RA, Qin Y, Srikantan S, Morales NP, Li Q, Deng Y, Kim SW, Pereira MA, Toledo SP, and Su X, et al (2013). In vivo and in vitro oncogenic effects of HIF2A mutations in pheochromocytomas and paragangliomas. *Endocr Relat Cancer* **20**, 349–359.

[27] Shankavaram U, Fliedner SM, Elkahloun AG, Barb JJ, Munson PJ, Huynh TT, Matro JC, Turkova H, Linehan WM, and Timmers HJ, et al (2013). Genotype and tumor locus determine expression profile of pseudohypoxic pheochromocytomas and paragangliomas. *Neoplasia* **15**, 435–447.

[28] Holmquist-Mengelbier L, Fredlund E, Lofstedt T, Noguera R, Navarro S, Nilsson H, Pietras A, Vallon-Christersson J, Borg A, and Gradin K, et al (2006). Recruitment of HIF-1alpha and HIF-2alpha to common target genes is differentially regulated in neuroblastoma: HIF-2alpha promotes an aggressive phenotype. *Cancer Cell* **10**, 413–423.

[29] Schodel J, Oikonomopoulos S, Ragoussis J, Pugh CW, Ratcliffe PJ, and Mole DR (2011). High-resolution genome-wide mapping of HIF-binding sites by ChIP-seq. *Blood* **117**, e207–e217.

[30] Keith B, Johnson RS, and Simon MC (2012). HIF1alpha and HIF2alpha: sibling rivalry in hypoxic tumour growth and progression. *Nat Rev Cancer* **12**, 9–22.

[31] Yusuf D, Butland SL, Swanson MI, Bolotin E, Ticoll A, Cheung WA, Zhang XY, Dickman CT, Fulton DL, and Lim JS, et al (2012). The transcription factor encyclopedia. *Genome Biol* **13**, R24.

[32] Camenisch G, Wegner RH, and Peso L (2012). In: Yusuf D, editor. HIF1A, vol. 13. Genome Biol; 2012. p. R24.

[33] Olechnowicz SWZ and Peet DJ (2012). In: Yusuf D, editor. EPAS1, vol. 13. Genome Biol; 2012. p. R24.

[34] Benita Y, Kikuchi H, Smith AD, Zhang MQ, Chung DC, and Xavier RJ (2009). An integrative genomics approach identifies hypoxia inducible factor-1 (HIF-1)-target genes that form the core response to hypoxia. *Nucleic Acids Res* **37**, 4587–4602.

[35] Richter S, Qin N, Pacak K, and Eisenhofer G (2013). Role of hypoxia and HIF2alpha in development of the sympathoadrenal cell lineage and chromaffin cell tumors with distinct catecholamine phenotypic features. *Adv Pharmacol* **68**, 285–317.

[36] Favier J, Igaz P, Burnichon N, Amar L, Libe R, Badoual C, Tissier F, Bertherat J, Plouin PF, and Jeunemaitre X, et al (2012). Rationale for anti-angiogenic therapy in pheochromocytoma and paraganglioma. *Endocr Pathol* **23**, 34–42.

[37] Towle R, Truong D, Hogg K, Robinson WP, Poh CF, and Garnis C (2013). Global analysis of DNA methylation changes during progression of oral cancer. *Oral Oncol* **49**, 1033–1042.

[38] Daino K, Ugolin N, Altmeyer-Morel S, Guilly MN, and Chevillard S (2009). Gene expression profiling of alpha-radiation–induced rat osteosarcomas: identification of dysregulated genes involved in radiation-induced tumorigenesis of bone. *Int J Cancer* **125**, 612–620.

[39] Jain R, Fischer S, Serra S, and Chetty R (2010). The use of cytokeratin 19 (CK19) immunohistochemistry in lesions of the pancreas, gastrointestinal tract, and liver. *Appl Immunohistochem Mol Morphol* **18**, 9–15.

[40] Skondra M, Gkioka E, Kostakis ID, Pissimissis N, Lembessis P, Pectasides D, and Koutsilieris M (2014). Detection of circulating tumor cells in breast cancer patients using multiplex reverse transcription-polymerase chain reaction and specific primers for MGB, PTHRP and KRT19 correlation with clinicopathological features. *Anticancer Res* **34**, 6691–6699.

[41] Loriot C, Burnichon N, Gadessaud N, Vescovo L, Amar L, Libe R, Bertherat J, Plouin PF, Jeunemaitre X, and Gimenez-Roqueplo AP, et al (2012). Epithelial to mesenchymal transition is activated in metastatic pheochromocytomas and paragangliomas caused by SDHB gene mutations. *J Clin Endocrinol Metab* **97**, E954-962.

[42] Loriot C, Domingues M, Berger A, Menara M, Ruel M, Morin A, Castro-Vega LJ, Letouze E, Martinelli C, and Bemelmans AP, et al (2015). Deciphering the molecular basis of invasiveness in Sdhb-deficient cells. *Oncotarget* **6**, 32955–32965.

[43] Fliedner SM, Kaludercic N, Jiang XS, Hansikova H, Hajkova Z, Sladkova J, Limpuangthip A, Backlund PS, Wesley R, and Martiniova L, et al (2012). Warburg effect's manifestation in aggressive pheochromocytomas and paragangliomas: insights from a mouse cell model applied to human tumor tissue. *PLoS One* **7**, e40949.

[44] Hervouet E, Demont J, Pecina P, Vojtiskova A, Houstek J, Simonnet H, and Godinot C (2005). A new role for the von Hippel–Lindau tumor suppressor protein: stimulation of mitochondrial oxidative phosphorylation complex biogenesis. *Carcinogenesis* **26**, 531–539.

[45] Hervouet E, Cizkova A, Demont J, Vojtiskova A, Pecina P, Franssen-van Hal NL, Keijer J, Simonnet H, Ivanek R, and Kmoch S, et al (2008). HIF and reactive oxygen species regulate oxidative phosphorylation in cancer. *Carcinogenesis* **29**, 1528–1537.

[46] Goffrini P, Ercolino T, Panizza E, Giache V, Cavone L, Chiarugi A, Dima V, Ferrero I, and Mannelli M (2009). Functional study in a yeast model of a novel succinate dehydrogenase subunit B gene germline missense mutation (C191Y) diagnosed in a patient affected by a glomus tumor. *Hum Mol Genet* **18**, 1860–1868.

[47] Chang YL, Hsieh MH, Chang WW, Wang HY, Lin MC, Wang CP, Lou PJ, and Teng SC (2015). Instability of succinate dehydrogenase in SDHD polymorphism connects reactive oxygen species production to nuclear and mitochondrial genomic mutations in yeast. *Antioxid Redox Signal* **22**, 587–602.

[48] Huang J and Lemire BD (2009). Mutations in the *C. elegans* succinate dehydrogenase iron-sulfur subunit promote superoxide generation and premature aging. *J Mol Biol* **387**, 559–569.

[49] Biswas S, Troy H, Leek R, Chung YL, Li JL, Raval RR, Turley H, Gatter K, Pezzella F, and Griffiths JR, et al (2010). Effects of HIF-1alpha and HIF2alpha on growth and metabolism of clear-cell renal cell carcinoma 786-0 xenografts. *J Oncol* **2010**, 757908.

[50] Chiavarina B, Martinez-Outschoorn UE, Whitaker-Menezes D, Howell A, Tanowitz HB, Pestell RG, Sotgia F, and Lisanti MP (2012). Metabolic reprogramming and two-compartment tumor metabolism: opposing role(s) of HIF1alpha and HIF2alpha in tumor-associated fibroblasts and human breast cancer cells. *Cell Cycle* **11**, 3280–3289.

[51] Yang C, Zhuang Z, Fliedner SM, Shankavaram U, Sun MG, Bullova P, Zhu R, Elkahloun AG, Kourlas PJ, and Merino M, et al (2015). Germ-line PHD1 and PHD2 mutations detected in patients with pheochromocytoma/paraganglioma-polycythemia. *J Mol Med* **93**, 93–104.

[52] Liu L, Cash TP, Jones RG, Keith B, Thompson CB, and Simon MC (2006). Hypoxia-induced energy stress regulates mRNA translation and cell growth. *Mol Cell* **21**, 521–531.

[53] Zhao WT, Zhou CF, Li XB, Zhang YF, Fan L, Pelletier J, and Fang J (2013). The von Hippel–Lindau protein pVHL inhibits ribosome biogenesis and protein synthesis. *J Biol Chem* **288**, 16588–16597.

[54] Romero-Ruiz A, Bautista L, Navarro V, Heras-Garvin A, March-Diaz R, Castellano A, Gomez-Diaz R, Castro MJ, Berra E, and Lopez-Barneo J, et al (2012). Prolyl hydroxylase–dependent modulation of eukaryotic elongation factor 2 activity and protein translation under acute hypoxia. *J Biol Chem* **287**, 9651–9658.

[55] Mizuta K, Sakabe M, Hashimoto A, Ioka T, Sakai C, Okumura K, Hattammaru M, Fujita M, Araki M, and Somekawa S, et al (2015). Impairment of endothelial-mesenchymal transformation during atrioventricular cushion formation in Tmem100 null embryos. *Dev Dyn* **244**, 31–42.

[56] Ou D, Yang H, Hua D, Xiao S, and Yang L (2015). Novel roles of TMEM100: inhibition metastasis and proliferation of hepatocellular carcinoma. *Oncotarget* **6**, 17379–17390.

[57] Cleary S, Phillips JK, Huynh TT, Pacak K, Elkahloun AG, Barb J, Worrell RA, Goldstein DS, and Eisenhofer G (2007). Neuropeptide Y expression in phaeochromocytomas: relative absence in tumours from patients with von Hippel–Lindau syndrome. *J Endocrinol* **193**, 225–233.

[58] Fliedner SM, Breza J, Kvetnansky R, Powers JF, Tischler AS, Wesley R, Merino M, Lehnert H, and Pacak K (2010). Tyrosine hydroxylase, chromogranin A, and steroidogenic acute regulator as markers for successful separation of human adrenal medulla. *Cell Tissue Res* **340**, 607–612.